VNU Journal of Science: Mathematics - Physics
Journal homepage: https://js.vnu.edu.vn/MaP

Original Article

Effect of Sr Content on Microstructure and Electrical Properties of Lead-free $Ba_{1-x}Sr_xTiO_3$ thin Films

Vu Thu Hien[1,*], Nguyen Thi Minh Phuong[1,2], Vu Ngoc Hung[1]

[1]*Falculty of Electronic Materials and Devices, Hanoi University of Science and Technology, 1 Dai Co Viet, Hai Ba Trung, Hanoi, Vietnam*

[2]*University of Transport Technology, 54 Trieu Khuc, Thanh Xuan, Hanoi, Vietnam*

Received 22nd October 2024
Revised 29th November 2024; Accepted 10th March 2025

Abstract: Lead-free barium titanate based $Ba_{1-x}Sr_xTiO_3$ thin films ($x = 0 \div 0.45$) have been deposited onto $Pt/Ti/SiO_2/Si(100)$ substrate *via* sol–gel technique. The films were crystallized at temperature of 650 °C for 30 min in the air. The experimental data displayed that microstructure, dielectric and ferroelectric properties of the films were strongly influenced by the Sr concentration. All the films are well formed in a polycrystalline perovskite phase with a shift of diffraction planes toward larger 2θ as increasing Sr content. High resolution scanning electron microscopy images as well as cross-section profile indicate a dense structure, clear grains and a sharp interface between the film and Pt electrode. However, the shape and grain size change among Sr-doped films. Series data on capacitance - voltage measurements reveal that dielectric constant (ε) increases with Sr-dopant concentration while loss tangent (tanδ) decreases. The optimal dielectric properties are found for $Ba_{0.55}Sr_{0.45}TiO_3$ (x= 0.45), while $Ba_{0.65}Sr_{0.35}TiO_3$ (x= 0.35) thin films perform better polarization properties with the maximum polarization of 8.07 $\mu C/cm^2$ under applied electric field of 1,000 kV/cm.

Keywords: Lead-free BST-BZT thin film, chemical solution deposition, microstructure, dielectrics

1. Introduction

During the past decades, traditional lead zirconate-titanate $Pb(Zr,Ti)O_3$ (PZT) is a common piezoelectric material that has been used for preparation of electromechanical devices [1]. However, the high toxicity of lead to the health and environment resulting to the lead-based piezoelectrics are being replaced with lead-free alternatives [2]. Therefore, lead-free ferroelectrics, currently, withdraw a lot of research attention. Among the ferroelectric materials, barium titanate based $Ba_{1-x}Sr_xTiO_3$ (BST)

* Corresponding author.
E-mail address: hienvt@itims.edu.vn

https//doi.org/10.25073/2588-1124/vnumap.4974

with distinct perovskite crystalline structure ABO_3 is a promising candidate for microelectronic devices such as nonvolatile random access memory, motion and thermal sensors, phase shifter, tunable microwave and energy storage devices due to its high dielectric constant and relatively low dielectric loss in a wide frequency range [3-5]. Essentially, BST is a solid solution of ferroelectric $BaTiO_3$ and paraelectric $SrTiO_3$. According to the results reported in [6, 7], the polarization and dielectric properties of these materials are dependent on both the off-center displacement of Ti atom from the elementary-cell octahedron [BO_6] and the type of cation A. On the other hand, to develop these materials for practical application, the preparation of high-quality BST as well as improving its electrical properties are very important. It has been known from the review articles over the past few years that Curie temperature (T_C) and dielectric properties of BST can be tailored by inserting Sr element into Ba site and changing Ba/Sr atom ratio. $Ba_{1-x}Sr_xTiO_3$ is attributed to be ferroelectric and paraelectric when x is in range of 0 ÷ 0.3 and 0.4 ÷ 1, respectively [8, 9]. Values of dielectric constant and dielectric loss with composition reported by various research groups present a wide variation. In general, the optimal permittivity is found for BST thin films with the composition x ranging from 0.4 to 0.5 [10-12]. Moreover, variations in dielectric constant and dielectric loss are reported differently for different thin film composition as well as different thickness and deposition conditions. Therefore, to study the influence of composition, thin films with different composition need to be fabricated under similar technological conditions.

In the present work, BST (x= 0 ÷ 0.45) thin films were deposited from modified precursor solutions by the costly effective sol–gel process onto $Pt/Ti/SiO_2/Si(100)$ substrates. The effect of Sr/Ba composition in a precursor solution on the phase structure, the surface morphology, and the electrical properties of the resultant BST thin films was investigated and discussed.

2. Experimental Details

Raw initiative materials utilized in this work include barium acetate [$(CH_3COO)_2Ba$, ACS reagent 99%, Sigma-Aldrich], strontium acetate [$(CH_3COO)_2Sr$, purity 98%, Sigma-Aldrich], titanium(IV)-isopropoxide [$C_{12}H_{28}O_4Ti$, 98%, Merck] and zirconium(IV)-propoxide [$(C_{12}H_{28}O_4)Zr$, 70% in 1-propanol, Acros]. Glacial acetic acid (CH_3COOH), 2-methoxy ethanol (2-MOE), and acetylacetone ($C_5H_8O_2$) were used as the solvent, and chelating agent, respectively. The desired moll ratio of Ba/Sir according to $Ba_{1-x}Sr_xTiO_3$ (x=0, 0.25, 0.35, and 0.45 denoted as BT, B75, B65 and B55, respectively) were weighted and dissolved completely in acetic acid with constant stirring at 120 ^oC for 5 hours to form salt precursor. Then, titanium(IV)-isopropoxide and 2-MOE were added into the solution while keeping continuous stirring at 80 ^oC for at least 3 hours to obtain BT, B75, B65 and B55 precursors, respectively. In those solutions acetylacetone was added to stabilize the solution. Various precursors of BT, B75, B65 and B55 with a fixed concentration of 0.40 M were prepared for depositing thin film.

All thin films were spin-coated onto $Pt/Ti/SiO_2/Si(100)$ substrates with the rate of 3,000 rpm for 30 s. The as-coated films were dried at 150 ^oC for 5 min, then at 450 ^oC for 10 min using a tube furnace (TF55030C, Linberg/Blue M). Heating speed selected for the whole temperature processing was 10 ^oC per min. These steps were repeated five to ten times to achieve a desired film thickness. Finally, the films were annealed at 650 ^oC for 30 min in air to form perovskite phase.

The crystalline phase and crystallographic orientation of the film were examined by using XRD method (XRD; Bruker, Germany). The surface morphology and thickness of the films were evaluated by Field emission scanning electron microscopy (FE-SEM, HELIOS 650, USA). For electrical measurements, ~ 100 nm-thick Pt top-electrodes were sputtered on the surface of the films *via* a Cr-mask and lift-off lithography process to form metal–insulator–metal (MIM) capacitors. Squared-pad sizes of 30×30, 100×100, 150×150, and 200×200 μm^2 were produced. Capacitance measurement and hysteresis loop were examined by TF Analyzer 2000 (aix ACCT, Germany). All the measurements were carried-out at room temperature.

3. Results and Discussion

3.1. Microstructural Properties

From XRD it is seen that the as-deposited films were amorphous, wheeas in the films either crystallized at temperatures larger 700 °C or spin-coated over 12 coating layers severely appeared cracks. Therefore, the samples were prepared only with 10 coating layers and thenannealed at 650 °C.

Four XRD patterns of BT, and BT-based thin films with different Sr content in a range of 2θ from 20^o to 75^o are presented in Fig. 1. It can be seen that all the films exhibited well crystallinity. Besides the peaks of Pt bottom electrode and Si substrate, all XRD patterns have basically well-defined diffraction planes, including (100), (110), (200), (210) and (211) which relate to tetragonal perovskite structures [13, 14]. The most intense reflections are of (110) and (210) peaks. B75 and B55 films show peaks around 24^o and 28.8^o among the perovskite peaks. The small amount of the second phase is attributed to be $BaCO_3$ or $(Ba,Sr)_2TiO_4$ phases [15, 16].

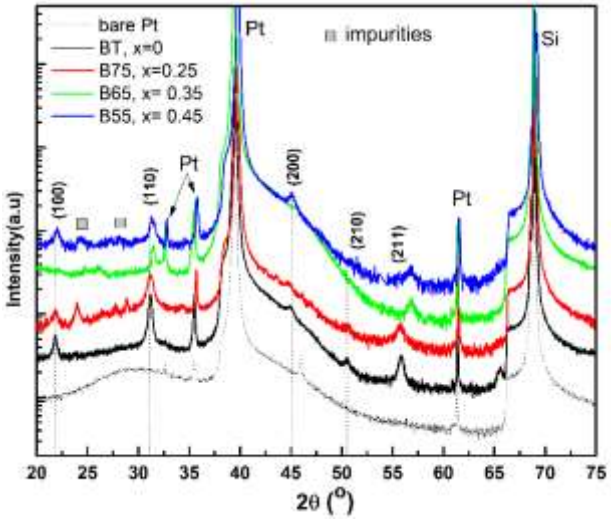

Figure 1: X-Ray diffraction pattern of barium titanate thin films with various Sr content annealed at 650 ^{o}C/30 min in the air. The Miller indices of the main phase peaks and the peak positions of Pt electrode and Si substrate as reference are indicated.

It is note that the diffraction peaks shift toward larger diffraction angles as the Sr content increases from 0 to 0.45, which implies the change in the lattice constant due to the partial substitution of Sr^{2+} into $BaTiO_3$ lattice. In comparison to pure BT, the parameters of the unit cell of B75, B65 and B55 may be reduced because the radius ion of Sr^{2+} (0.113 nm) is smaller than that of Ba^{2+} (0.135 nm) [17-19].

The 2θ peak shift is most obviously observed at (100), (110) and (211) planes. Fig. 2 displays two representative XRD patterns of the (110) and (211) peaks as a function of Sr content. These diffraction peaks are achieved in the range of 2θ from 30° to 32° and from 54° to 58°determined by analyzing the individual peak using Gauss curve fit function. As observed from the shape of the XRD patterns, the fitting procedure yields a significant decrease of the tetragonal phase content with increase in Sr amount (Table 1). The results showed that not only the unit cell change but the crystalline grain size also seems to be decreased since the full width at half maximum (FWHM) of B75, B65 and B55 increases.

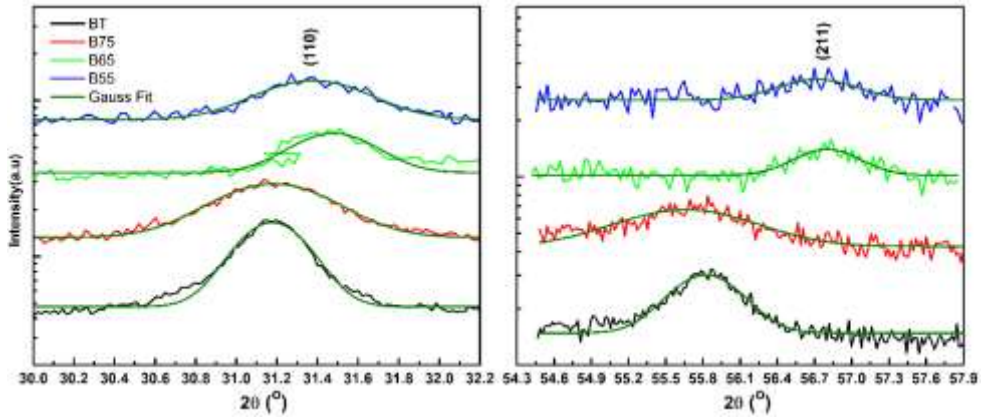

Figure 2: XRD profile around 30° to 32° (left) and 54° to 58° (right).

Table 1. 2θ and FWHM estimated from (100), (110) and (211) diffraction peaks of BT, B75, B65 and B55 thin films

Planes (hkl) / Samples	(100)		(110)		(211)	
	2θ (degree)	FWHM	2θ (degree)	FWHM	2θ (degree)	FWHM
BT, x=0	21.83	0.389	31.18	0.408	55.82	0.673
B75, x=0.25	21.82	0.408	31.18	0.672	55.66	1.266
B65, x= 0.35	--	--	31.48	0.477	56.80	0.600
B55, x= 0.45	22.00	0.513	31.38	0.620	56.72	0.633

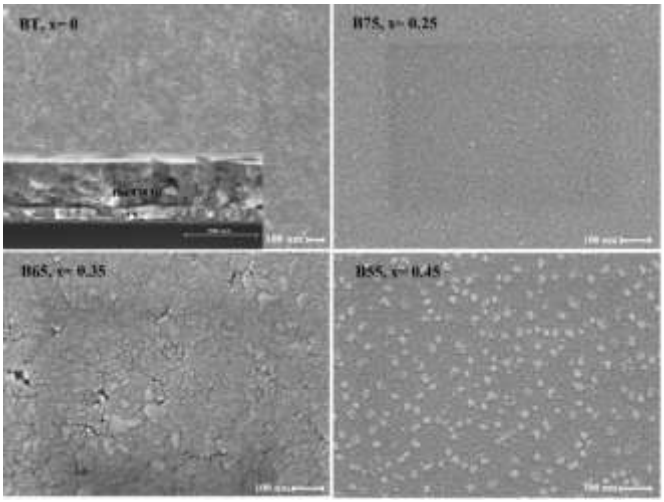

Figure 3: SEM images of the top surface of spin-coated BT, B75, B65 and B55 thin films on Pt electrode. Insert image show cross-section of BT film. The thickness of 10L BT film is 402 nm, which turns to around 40 nm per a coating layer.

Fig. 3 shows typical SEM images of the surface and cross-sectional morphologies of BT, B75, B65 and B55 thin films. These films are rather dense, smooth and there are no crack. However, the of Ba/Sr ratio significantly affects to the grain shape and size. BT films show granular shape with the size of 35

- 100 nm. Meanwhile, the Sr-doped films give particles of round shape and rather small size. Similar behavior has been reported for CSD and PLD derived BST and BSZT thin films with a smaller grain sizes [17, 20]. Slight deviation in the grain size with increase of Sr/Ba content is explained due to non-uniform agglomerates during the process. During annealing, the nucleation as well as the grain growth process for the different composition in the perovskite materials occurred differently [7]. The grain size of the film shows a little change with the increase of the Sr concentration. Grains with slightly increased size and improved crystalline structure are observed clearer for the sample B55, then B65, and B75.

Surface mapping for BT is confirmed by cross-sectional analysis shown in the insert image in Fig. 3. One can see that the out-of-plane grain sizes and morphologies are similar to the top surface: the grains are granular and dense. The total thickness of the BT film is *ca*. 402 nm for 10 coating layers, which turns out ~ 40 nm per coating layer.

3.2. Dielectric and Ferroelectric Properties

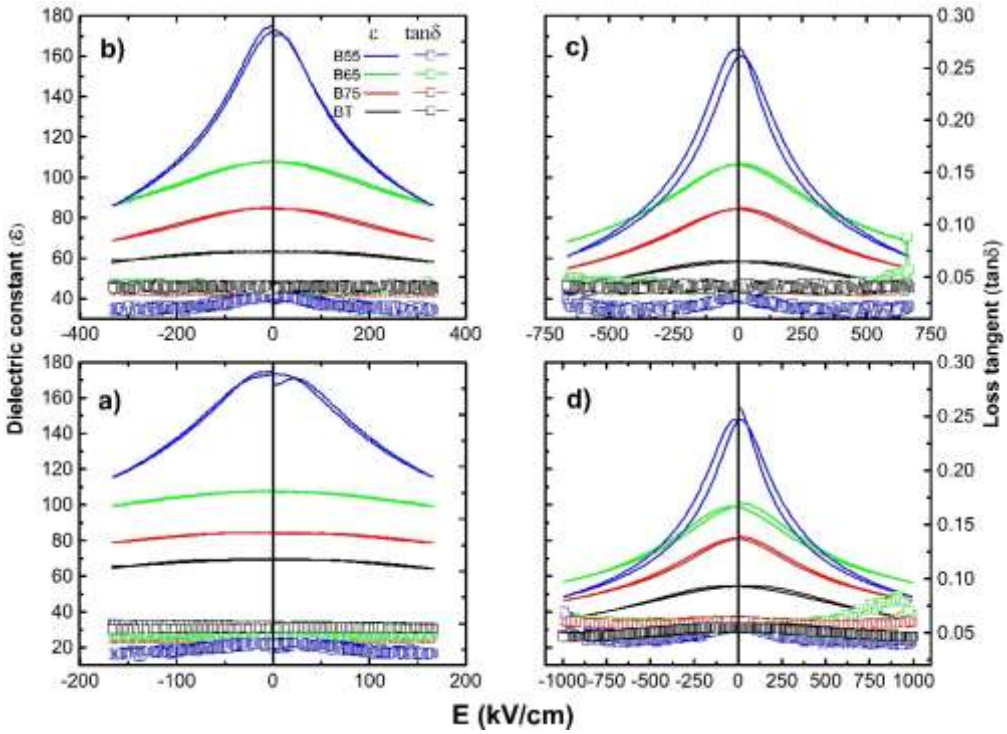

Figure 4: Dielectric constant and loss tangent of BT, B75, B65 and B55 thin films measured at different applied voltage ranges: (a) ± 5V; (b) ± 10V; (c) ± 20V and (d) ± 30V.

Sr/Ba ratio dependence of the dielectric constant and dielectric loss as function of applied electric field is given in Fig. 4. Typical butterfly shape of the ε-E curves is observed at almost applied electric field range for all thin films, which indicates the presence of ferroelectric phase as expected from XRD measurements. Furthermore, with the increasing in the electric field, the relative permittivity decreases and dielectric loss slightly increases. The $Ba_{0.55}Sr_{0.45}TiO_3$ (B55) thin film always possesses the largest dielectric constant and the ε decreases with decreasing Sr content down to x = 0. The dielectric constant at 100 kHz and zero bias for different applied voltage ranges and different Sr compositions are listed in the Table 2. B55 thin films also exhibit the lowest tanδ (~ 0.026) and B75 hold the largest one (~ 0.062).

The obtained results are probably related to the grain size effect among the doped-Sr thin films as seen in SEM images.

Table 2. Dielectric constant and loss tangent of BT, B75, B65 and B55 thin films

Voltage range (V)	Dielectric constant, ε at bias = 0V				Dielectric loss, tanδ at bias = 0V			
	BT, x= 0	B75, x= 0.25	B65, x= 0.35	B55, x= 0.45	BT, x= 0	B75, x= 0.25	B65, x= 0.35	B55, x= 0.45
± 5	69.60	84.62	108.05	174.60	0.046	0.036	0.039	0.026
± 10	63.42	85.30	108.00	174.43	0.041	0.042	0.036	0.029
± 20	58.41	80.00	107.10	164.45	0.042	0.040	0.040	0.031
± 30	54.45	82.40	101.32	155.52	0.054	0.062	0.061	0.058

Finaly, the ferroelectric nature of three doped-Sr (B75, B65 and B55) thin films was examined by a hysteresis loop of polarization (P) as a function of an applied electric field (E) at 1 kHz. The obtained (P-E) curves are depicted in Fig. 5. All the films show rather narrow (P-E) loops at low applied voltage ranges (5 and 10V),

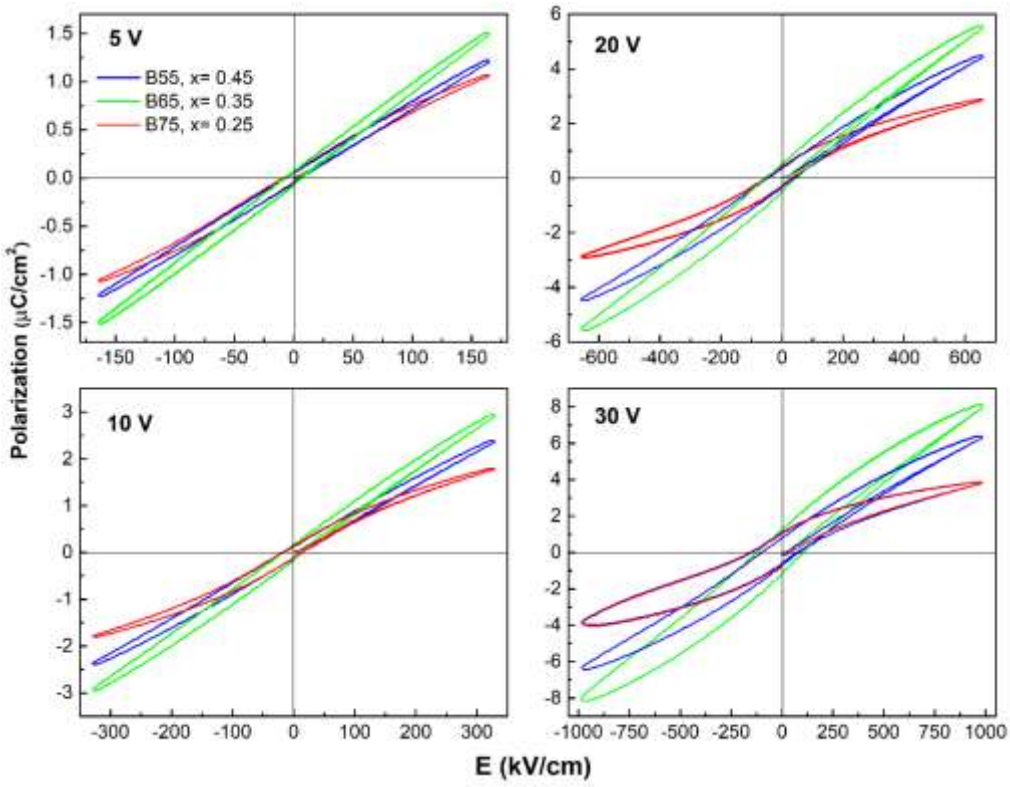

Figure 5. Hysteresis loops of $Ba_{1-x}Sr_xTiO_3$ (x= 0.25; 0.35 and 0.45) thin films performed at frequency of 1 kHz and different voltage ranges.

while a better-defined hysteresis loop is achieved at higher voltages, *e.g.* 20 and 30V. The ferroelectric properties of barium titanate based thin films significantly depend on Sr composition. Such effect is obviously found on the maximum polarization, P_{max} and coercive field, E_c (Fig. 6). According to Fig. 6, the highest and lowest values of P_{max} are found on B65 and B75 films, respectively. Meanwhile in most

case, B55 thin films show the lowest E_c, which implies that ferroelectric domains in B55 are more easily polarized. The decrease in P_{max} can be attributed to smaller grain size in B75 thin film, which inhibited the formation of large ferroelectric domains, then reduced the effective contribution to total polarization. As a consequence of inhibition, the polarization becomes weaker. The maximum polarization is well retained up to 8.07 μC/cm^2 for x = 0.35, but it degraded close to 3.84 μC/cm^2 for x = 0.25.

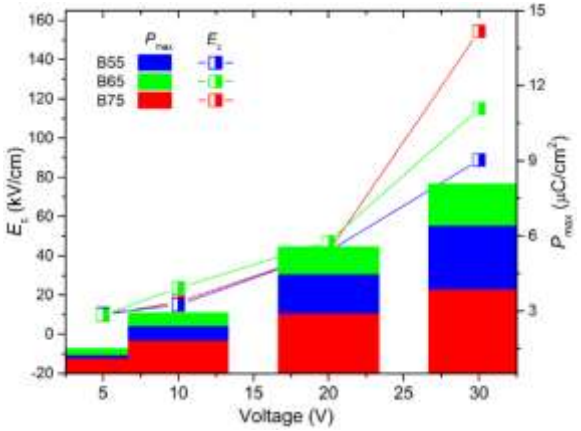

Figure 6. Values of P_{max} and E_c estimated from P-E loops of B75, B65 and B55 thin films.

4. Conclusion

In summary, the composition influence on the microstructure and dielectric/ferroelectric properties of Sr-doped $Ba_{1-x}Sr_xTiO_3$ (x= 0, 0.25, 0.35 and 0.45) thin films coated on Pt/Ti/SiO_2/Si(100) substrates from a simply effective sol–gel method has been studied. It was revealed that the diffraction peaks shifted to the låger 2θ angles with the addition of Sr. All the films show granular, none of cracks and dense surface. However, the shape and size of grains change slightly increased as increasing Sr/Ba ratio. Such effect of microstructural change has impacted differently on the dielectric and ferroelectric properties of those BT-based films. The optimal dielectric properties with largest dielectric constant and lowest dielectric loss has been found for $Ba_{0.55}Sr_{0.45}TiO_3$ (B55) thin films, while $Ba_{0.65}Sr_{0.35}TiO_3$ (B65) thin films have better polarization properties.

Acknowledgments

The authors acknowledge the financial support by the Ministry of Education and Training (MOET) under Grant number B2023-BKA-20.

References

[1] N. Setter, D. Damjanovic, L. Eng, G. Fox, S. Gevorgian, S. Hong, A. Kingon, H. Kohlstedt, N. Y. Park, G. B. Stephenson, I. Stolitchnov, A. K. Taganstev, D. V. Taylor, T. Yamada, S. Streiffer, FerroelectricThin Films: Review of Materials, Properties, and Applications, Journal of Applied Physics, Vol. 100, No. 5, 2006, pp. 051606-051646, https://doi.org/10.1063/1.2336999.

[2] T. H. E. E. Parliament, T. H. E. Council, O. F. The, E. Union, Restriction of The Use of Certain Hazardous Substances in Electrical and Electronic Equipment (RoHS), Official Journal European Union, Vol. 54, 2011, pp. L174/88-L174/110, https://doi.org/10.3000/17252555.L_2011.174.eng.
[3] P. Bao, T. J. Jackson, X. Wang, M. J. Lancaster, Barium Strontium Titanate Thin Film Varactors for Room-Temperature Microwave Device Applications, Journal Physics D: Applied Physics, Vol. 41, No. 6, 2008, pp. 063001–063021, https://doi.org/10.1088/0022-3727/41/6/063001.
[4] A. Khalfallaoui, G. Velu, L. Burgnies, J. C. Carru, Characterization of Doped BST Thin Films Deposited by Sol-gel for Tunable Microwave Devices, IEEE Transactions on Ultrasonics, Ferroelectrics and Frequency Control, Vol. 57, 2009, pp. 295-298, https://doi.org/10.1109/FREQ.2009.5168189.
[5] S. U. Adikary, H. L. W. Chan, Compositionally Graded $Ba_xSr_{1-x}TiO_3$ Thin Films for Tunable Microwave Applications, Material Chemistry Physics, Vol. 79, No. 2–3, 2003, pp. 157-160, https://doi.org/10.1016/S0254-0584(02)00255-9.
[6] V. Polinger, I. B. Bersuker, Pseudo Jahn-Teller Effect in Permittivity of Ferroelectric Perovskites, Journal of Physics Conference Series, Vol. 833, 2017, pp. 012012, https://doi.org/10.1088/1742-6596/833/1/012012.
[7] A. Debnath, S. K. Lalwani, S. Singh, Sunny, Improvement in Ferroelectric Properties of $BaTiO_3$ Film by Mn/Sr Doping for Non-volatile Memory Applications, Micro and Nanostructures, Vol. 171, 2022, pp. 207421, https://doi.org/10.1016/j.micrna.2022.207421.
[8] S. W. Kim, H. I. Choi, M. H. Lee, J. S. Park, D. J. Kim, D. Do, M. H. Kim, T. K. Song, W. J. Kim, Electrical Properties and Phase of $BaTiO_3$-$SrTiO_3$ Solid Solution, Ceramics International, Vol. 39, 2013, pp. S487-S490, https://doi.org/10.1016/j.ceramint.2012.10.119.
[9] Y. Yu, H. Zou, Q. F. Cao, X. S. Wang, Y. X. Li, X. Yao, Phase Transitions and Relaxation Behaviors in Barium Strontium Titanate Ceramics Determined by Dynamic Mechanical and Dielectric Analysis, Ferroelectrics, Vol. 487, 2015, pp. 77-85, https://doi.org/10.1080/00150193.2015.1070641.
[10] L. C. Sengupta, S. Sengupta, Breakthrough Advances in Low Loss, Tunable Dielectric Materials, Material Research Innovations, Vol. 2, 1999, pp. 278-282, https://doi.org/10.1007/s100190050098.
[11] C. S. G. Derived, M. C. Gust, L. A. Momoda, N. D. Evans, M. L. Mecartney, Crystallization of Sol–Gel-Derived Barium Strontium Titanate Thin Films, Journal American Ceramic Society, Vol. 92, 2001, pp. 1087–1092, https://doi.org/10.1111/j.1151-2916.2001.tb00794.x.
[12] N.Y. Chan, D.Y. Wang, Y. Wang, J.Y. Dai, H.L.W. Chan, The Structural and In-plane Dielectric/Ferroelectric Properties of The Epitaxial $(Ba,Sr)(Zr,Ti)O_3$ Thin Films, Journal Applied Physics, Vol. 115, 2014, pp. 0-7, https://doi.org/10.1063/1.4883963.
[13] B. D. Stojanovic, A. Z. Simoes, C. O. Paiva-Santos, C. Jovalekic, V. V. Mitic, J. A. Varela, Mechanochemical Synthesis of Barium Titanate, Journal European Ceramic Society, Vol. 25, 2005, pp. 1985-1989, https://doi.org/10.1016/j.jeurceramsoc.2005.03.003.
[14] P. T. M. Nguyen, T. Nguyen, M. D. Nguyen, T. Vu, Impact of Electrode Materials on Microstructure, Leakage Current and Dielectric Tunable Properties of Lead-free BSZT Thin Films, Ceramics International, Vol. 47, 2021, pp. 23214-23221, https://doi.org/10.1016/j.ceramint.2021.05.033.
[15] W. C. Zhu, D. W. Peng, J. R. Cheng, Z. Y. Meng, Effect of (Ba+Sr)/Ti Ratio on Dielectric and Tunable Properties of $Ba_{0.6}Sr_{0.4}TiO_3$ Thin Film Prepared by Sol-gel Method, Transactions of Nonferrous Metal Society of China, Vol. 16, 2006, pp. s261–s265, https://doi.org/10.1016/S1003-6326(06)60187-8.
[16] V. R. Mudinepalli, L. Feng, W. C. Lin, B.S. Murty, Effect of Grain Size on Dielectric and Ferroelectric Properties of Nanostructured $Ba_{0.8}Sr_{0.2}TiO_3$ Ceramics, Journal Advanced Ceramics, Vol. 4, No. 1, 2015, pp. 46-53, https://doi.org/10.1007/s40145-015-0130-8.
[17] S. Tinte, M. G. Stachiotti, S. R. Phillpot, M. Sepliarsky, D. Wolf, Ferroelectric and Dielectric Properties of Sol–gel Derived $Ba_xSr_{1-x}TiO_3$ Thin Films, Thin Solid Film, Vol. 424, 2003, pp. 70-74, https://doi.org/10.1016/S0040-6090(02)00918-5.
[18] M. Arshad, H. Du, M. S. Javed, A. Maqsood, I. Ashraf, S. Hussain, W. Ma, H. Ran, Fabrication, Structure, and Frequency-dependent Electrical and DielectricProperties of Sr-doped $BaTiO_3$ Ceramics, Ceramics International, Vol. 46, 2020, pp. 2238-2246, https://doi.org/10.1016/j.ceramint.2019.09.208.
[19] B. Vigneshwaran, P. Kuppusami, S. Ajithkumar, H. Sreemoolanadhan, Study of Low Temperature-dependent Structural, Dielectric, and Ferroelectric Properties of $Ba_xSr_{1-x}TiO_3$ (x=0.5, 0.6, 0.7) Ceramics, Journal of Materials Science: Materials in Electronics, Vol. 31, 2020, pp. 56, https://doi.org/10.1007/s10854-020-03593-3.
[20] N. Y. Chan, D. Y. Wang, Y. Wang, J. Y. Dai, H. L.W. Chan, The Structural and In-plane Dielectric/Ferroelectric Properties of The Epitaxial $(Ba,Sr)(Zr,Ti)O_3$ Thin Films, Journal Applied Physics, Vol. 115, 2014, pp. 234102, https://doi.org/10.1063/1.4883963.